Concepts for nanoscale resolution in fluorescence microscopy

Stefan W Hell[*], Marcus Dyba[1] and Stefan Jakobs[2]

Spatio-temporal visualization of cellular structures by fluorescence microscopy has become indispensable in biology. However, the resolution of conventional fluorescence microscopy is limited by diffraction to about 180 nm in the focal plane and to about 500 nm along the optic axis. Recently, concepts have emerged that overcome the diffraction resolution barrier fundamentally. Formed on the basis of reversible saturable optical transitions, these concepts might eventually allow us to investigate hitherto inaccessible details within live cells.

Addresses
Max Planck Institute for Biophysical Chemistry, Department of NanoBiophotonics, Am Fassberg 11, 37070 Göttingen, Germany
e-mail: hell@nanoscopy.de[*] or mdyba@gwdg.de[1] or sjakobs@gwdg.de[2]

Abbreviations
CCD   charge coupled device
FWHM   full-width-half maximum
RESOLFT reversible saturable optical (fluorescent) transition
STED   stimulated emission depletion

Introduction: the resolution issue

The observation of dynamic processes in live cells, ranging from vesicle fusions, and protein transport to the emergence and decay of calcium waves, to name a few, has tremendously increased our understanding of the underlying biochemical networks. Major driving forces behind this development have been new imaging techniques in synergy with the generation of a plethora of fluorescent probes that make it possible to label membranes, organelles, and proteins with high specificity [1,2]. Although most specifically labeled cellular constituents can readily be detected in a conventional light microscope, their submicron scale structure cannot be perceived. For example, although many proteins of the inner mitochondrial membrane can be tagged with the green fluorescent protein (GFP), the cristae are too detailed to be represented in an image recorded with light.

Resolution is the minimal distance at which a microscope can distinguish between two or more features of the same

kind [3]. Therefore, resolution must not be confused with localization precision. Although it might easily be possible to localize with nanometer precision the center of the fluorescence patch generated by a membrane labeled synaptic vesicle in a microscope, its visualization as a 30–50 nm hollow sphere fails, because it requires nanometer scale resolution. In fact, conventional epifluorescence microscopy might not even resolve two synaptic vesicles touching each other. Similarly, it is possible to track the trajectory of a virus with nanometer precision but its inner structure remains elusive to light microscopy.

According to Abbe, the resolution limitation is ultimately rooted in the phenomenon of diffraction [3]. Loosely speaking, focusing of light always results in a blurred spot [4], whose size determines the resolution. The transverse (i.e. focal plane) full-width-at-half-maximum (FWHM) of the focal spot is quite precisely given by

$$\Delta x, \Delta y = \frac{\lambda}{2n \sin \alpha} \tag{1}$$

with λ, n, and α denoting the wavelength, the refractive index, and the semiaperture angle of the objective lens, respectively. In the main direction of light propagation (i.e. the optic axis), the spot size is about $\Delta z = 2\lambda/(n \sin^2 \alpha)$ [4].

In principle, the spatial resolution could be improved by employing shorter wavelengths and larger angles. However, this strategy ultimately faced quite stiff technical limits already a century ago. The most sophisticated modern immersion lenses provide a maximum angle of $\alpha=68°$; the shortest compatible wavelength for imaging live cells is around 400 nm, which is in the spectrum of near-UV light [5]. Thus, it seemed obvious that if visible light and regular lenses were to be used, the resolution in the focal plane $\Delta x, \Delta y$ would always be poorer than 150 nm [6]. Nevertheless, this is still better than the axial resolution of $\Delta z > 500$ nm.

Axial resolution improvement with opposing high angle lenses

The fact that the axial resolution is significantly poorer than its lateral counterpart indicates that there is room for improvement, even within the realm of diffraction. For the z-axis, the process of focusing is not optimal because there is an obvious asymmetry resulting from the main direction of light propagation. If the light field propagated from all directions towards the focal point, that is, if the converging wavefront encompassed a full solid angle of 4π, the focal spot would be (virtually) round. In this case, $\Delta x = \Delta y = \Delta z$, and the axial resolution would be similar to its lateral counterpart.

The creation of a complete spherical wavefront is technically difficult, if not impossible. But fortunately, this physical condition can be approximated by fusing the spherical wavefronts of two opposing lenses by interference [7,8]. Constructive interference at the focal point results in a pronounced intensity maximum that is ∼4 times narrower than that of a single lens. The lenses obviously have to be of a high numerical aperture [7,9]; the interference of flat counter-propagating wavefronts [10,11] is not suitable for unambiguous resolution increase along the optic axis [9,12].

The same consideration applies to the spherical wavefronts of the emerging fluorescence light [7]. They can also be added at the detector to nearly the same effect [13–15]. Because the two lenses cannot really make up a complete spherical wavefront of 4π solid angle, the sharp main maximum is accompanied by interference sidelobes, whose marked effects have to be eliminated by image processing (deconvolution) [16]. The challenge with this strategy of resolution improvement was (and still is) the definition of physical conditions that render the sharp maximum predominant over the sidelobes [17].

This challenge has so far been met with various types of (multiple) spot scanning 4Pi-microscopy [15,18–21] and with widefield I⁵M microscopy [22], albeit with some concessions. 4Pi-microscopy uses spherical wavefronts for fluorescence excitation (type A) or for both the excitation and the fluorescence collection (type C). I⁵M illuminates with flat standing waves and uses coherent high angle spherical wavefront collection [14]. With these approaches, an up to sevenfold improved axial resolution could be obtained along the optical axis [15,22]. I⁵M brings about convenient widefield detection, but also higher sidelobes that have so far restricted this technique to fixed cells. Being viable also with water immersion lenses [23], two-photon excitation 4Pi-microscopy is applicable to live cells, where it has been shown to provide an axial resolution of up to 80 nm [15]. Applications of 4Pi-microscopy include the 3D-representation of the mitochondrial network of live budding yeast cells [21], and that of the Golgi apparatus in live mammalian cells [24]. Meanwhile, 4Pi-microscopy has been developed into a commercial system featuring a dedicated 4Pi-optical module that is firmly interlaced with a state-of-the-art confocal scanning microscope (Leica, Mannheim, Germany) [15].

Shifting the diffraction resolution barrier by up to a factor of two

Because of its point like illumination and point like (i.e. spatially selective) detection, an ideal scanning confocal fluorescence microscope features a focal spot that is narrower in FWHM by a factor of 1.4 when compared to its epifluorescence counterpart [25]. The same holds true, of course, if the spatially selective detection is carried out (not by a pinhole but) with the pixels of a CCD-camera (charge coupled device-camera) [26]. In combination with suitable mathematical deconvolution, the resolution of a sequentially illuminating (i.e. scanning) fluorescence microscope can be improved up to a total factor of two when compared with conventional microscopy [27]. Sequential illumination might of course not only be carried out by scanning a single spot, as is the case in a standard confocal microscope, but also by scanning with multiple spots, or even by scanning with patterns [28–32]. Sequential illumination with patterns has been named 'structured illumination'. It offers the highest degree of parallelization, albeit at the expense of having to scan more often over the same spot in the sample. Besides, it also requires elaborate post-processing of the raw data. The suitability of the different approaches depends on the object features to be imaged. Although small objects next to large and extended ones (e.g. membranes) will be better resolved with a combination of single (or few) confocal point scanning with deconvolution, sequentially applied line patterns will be superior at imaging sparse objects [30].

The factor of improvement brought about by these established or more recent approaches ranges from 1.4 to 2.0 compared to conventional light microscopes. However, even under ideal conditions, without prior knowledge of the object, the gain in resolution can never exceed this factor of two. So while the values of $\Delta x, \Delta y$ and Δz would ideally be halved, their basic dependence on λ and α would still apply. In other words, scanning point or pattern illumination systems with spatially selective detection are limited by diffraction [17]. The diffraction barrier is not broken, but shifted.

Breaking of the diffraction barrier

A radical way of overcoming diffraction is to avoid focusing altogether. This is the basic idea of near-field optical microscopy [6,33,34]. In these types of microscopes, the interaction of light with the sample is confined by an ultra sharp tip. Alternatively, light is guided through a tiny aperture of subdiffraction size. The trade-off with these approaches is that they are confined to imaging surfaces, which makes them unsuitable for the 3D imaging of the interior of cells. This problem is aggravated by the need to control the position of a nanoscale-scanning tip with respect to a soft surface. Overcoming the limiting role of diffraction without having to overcome diffraction by itself is certainly more attractive, because it retains the advantages of non-contact imaging.

Since the inception of nonlinear optics a few decades ago [35], it has been clear that a nonlinear relationship between the applied intensity and the measured (fluorescence) signal would — at least in principle — expand the resolution capabilities of a focusing ('far-field') light microscope. However, this notion remained vague and

Figure 1
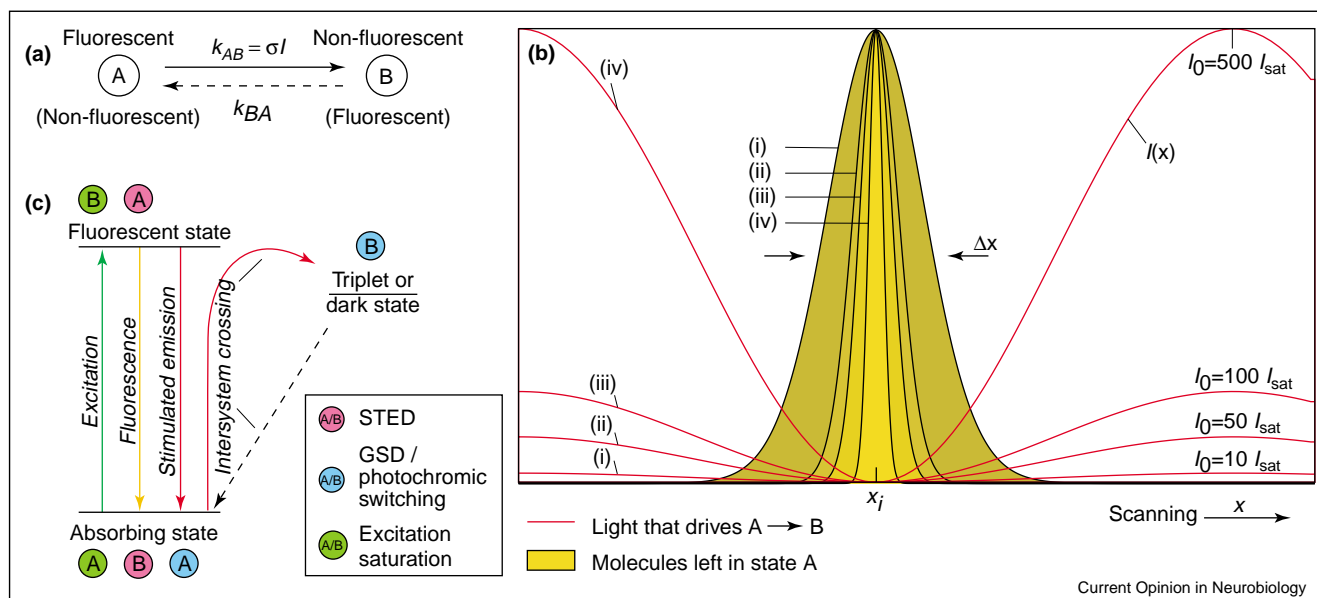
Breaking the diffraction barrier by reversible saturable optical transitions (RESOLFT). Breaking the diffraction barrier by RESOLFT requires **(a)** two states A and B of a label that are distinct in their optical properties. The optical transition A→B takes place at a rate $k_{AB} = \sigma I$ that is proportional to the light intensity I applied. The reverse transition B→A of rate k_{BA} brings the label back to its initial state. **(b)** The profiles i–iv show the spatial region in which the label is allowed to be in state A, if the region is subject to a standing wave of light with peak intensities I_0 = 10, 50, 100, and 500 times I_{sat} and with a zero intensity node at x_i. Increasing I_0 ensures that the region in which the label can reside in A is squeezed down, in principle, indefinitely. If A is the fluorescent state of the label, this ultrasharp region functions as the effective fluorescent spot of the microscope and Δx is the full-width-half-maximum of the state A region. The creation of a fluorescence image requires scanning, that is moving the zero node along the x-axis with subsequent storage of the recorded fluorescence. If B is the fluorescent state, then the ultrasharp regions of state A are dark. In this case, a sort of 'negative image' is recorded. Nevertheless, with suitable mathematical postprocessing, a similar optical resolution can be achieved. In any case, the resolution is no longer limited by diffraction, but only determined by the value of I_0/I_{sat}. **(c)** The simplified energy diagram of a fluorophore depicts possible schemes for implementing saturable optical transitions.

without consequence, because when examined in detail, most of the considered nonlinearities proved ineffective or even counterproductive to improving the resolution. In the early 1990s concrete physical concepts appeared for breaking the diffraction resolution barrier with focused light [36–38]. In fact, these concepts can be viewed as a family of concepts that utilize reversible saturable optical (fluorescence) transitions that we now term RESOLFT. They can be described in a common formalism [17].

Let us imagine a fluorescent molecule with two distinct states A and B, whereby the transition from A → B can be optically induced at a rate $k_{AB} = \sigma_{AB}I$ (Figure 1a). The variables σ_{AB} and I denote the transition cross-section and the light intensity, respectively. The rate for the reverse transition B → A is denoted with k_{BA}. It could be driven by light, by a chemical reaction, by heat, or by any other means, or simply be spontaneous. The kinetics of the molecular states are described by $dN_A/dt = -dN_B/dt = k_{BA}N_B - k_{AB}N_A$, with $N_{A,B}$ denoting the normalized population probability of each state. After a time period $t \gg (k_{AB} + k_{BA})^{-1}$, the populations have reached a dyna-

mical equilibrium at $N_A^\infty = k_{BA}/(k_{AB} + k_{BA})$. The probability of the molecule to be in A or B basically depends on k_{AB} and hence on I. At the 'saturation intensity' $I_{sat} = k_{AB}/\sigma_{BA}$, we have equal probability $N_A^\infty = 1/2$. Increasing $I \gg I_{sat}$ renders $k_{AB} \gg k_{BA}$, so that the molecule is virtually shifted to B: $N_A^\infty \to 0$.

Figure 1b illustrates how this behavior can be exploited for creating arbitrarily sharp regions of 'state A' molecules. The scheme in Figure 1b is one-dimensional (x), but can be readily extended to 3D. For this purpose we require the spatial intensity distribution $I = I(x)$ to be zero at a point x_i in space: $I(x_i) = 0$. Whereas in 2D or 3D, the light intensity distribution would be a 2D- or 3D-dough-nut-mode, in 1D the zero is best produced by a standing wave $I(x) = I_0\cos^2(2\pi n/\lambda)$. If we now apply $I(x)$ to a spatial distribution of molecules (in x) that are initially all in state A, for $I_0 \gg I_{sat}$, virtually all the molecules will be transferred to B, except for those that are closest in the vicinity of x_i. The larger the ratio $I_0/I_{sat} \gg 1$, the final region of state A; note the increase in the steepness of the curve with increasing saturation level I_0/I_{sat} in Figure 1b. The FWHM of the resulting spot of state A is readily

calculated as:

$$\Delta x \approx \frac{\lambda}{\pi n \sqrt{I_0/I_{sat}}} \tag{2}$$

In microscopy, the spatial distribution $I(x)$ can be produced by the objective lens itself. If it is produced through the finite aperture of the objective lens, the smallest possible spot is co-determined by the semiaperture angle:

$$\Delta x \approx \frac{\lambda}{\pi n \sin \alpha \sqrt{I_0/I_{sat}}} \tag{3}$$

that can be regarded as an extension of Abbe's equation (1) [17,39]. For $I_0/I_{sat} = 100$, the resolution improvement over Abbe is about tenfold. Despite the dependence of Δx on $\lambda/\sin \alpha$ and in contrast to equation (1), the new equations (2,3) allow diffraction-unlimited spatial resolution.

For a 3D-doughnut, we obtain a confined spatial volume of molecules in state A, whose dimensions decrease inversely with $\sqrt{I_0/I_{sat}}$. The reduction in volume scales with $(I_0/I_{sat})^{3/2}$, and for a given I_{sat} on the intensity I_0 that can be tolerated by the sample. Thus, in RESOLFT microscopy, the resolution is no longer limited by the wavelength λ, but by the applicable light intensity I at a given I_{sat} that is specific for the label.

If we now assume that state A but not state B is a fluorescent state, the relevance to imaging becomes obvious: our scheme allows us to create arbitrarily small fluorescence spots [17,37,39,40]. Moreover, by scanning the zero x_i across (or through) the specimen, we can record the fluorophore distribution point by point, and thus assemble a fluorescence 3D-image with arbitrary resolution. Within a framework of a RESOLFT microscopy concept, identical fluorescent objects can be separated in space irrespective of their proximity and size, because the fluorescence spot (state A) can be made so small that only one of the objects fluoresces.

The concept of RESOLFT inevitably requires scanning (with a zero), but not necessarily with a single beam or a point-like zero. Multiple zeros or dark lines [32,41] in conjunction with conventional CCD-camera detection can also be used, provided the zeros or the dark lines are further apart than the minimal distance required by the diffraction resolution limit of conventional CCD-camera imaging [17,32]. Dark lines increase the resolution in a single direction only, but rotating the pattern and subsequent computational reassignment [29,41] might provide, under some conditions, equally good subdiffraction resolution. The obligation for scanning remains. The need for scanning is also the reason why the saturable optical transition A→B has to be reversible. The molecule

in state B must be able to return to state A at the latest when the zero comes across its site.

Different approaches of RESOLFT microscopy

The RESOLFT scheme and the subsequent breaking of the diffraction barrier are the ideas behind stimulated emission depletion (STED) microscopy [36,37,42]. In STED-microscopy, molecules that have just been excited to the fluorescent state S_1 (state A) by an excitation pulse are immediately transferred by a second light pulse (with intensity I) to the molecular ground state S_0 (state B), so that fluorescence emission is prevented (Figures 1b,c and 2a). The physical effect responsible for this transfer is stimulated emission, a basic single-photon phenomenon that has the same cross-section as single-photon absorption ($\sigma \approx 10^{-16}$–10^{-18} cm^2). Because STED competes with the spontaneous fluorescence decay of $k_{fl} \approx (1 \, \text{ns})^{-1}$ of the S_1, the saturation intensity I_{sat} can be approximated as k_{fl}/σ. It amounts to 10^{25}–10^{27} photons per cm^2 and per second, that is, several tens to a hundred of MW/cm^2 (Figure 2b). Saturated depletion of the excited state with a focal spot containing a zero squeezes the extent of the fluorescent spot to a subdiffraction size that is not limited by the wavelength any longer but only by the applicable intensity. The potential and details of STED-microscopy will be discussed later.

Other concepts with different physical realizations of state A and B have also been suggested (Figure 1c; [40]). For example, in ground state depletion (GSD) microscopy [36,38], the ground state S_0 has the role of state A, whereas state B is a metastable triplet state; more precisely, A and B are the singlet and triplet systems of the dye, respectively. For several dyes, intersystem crossing (A→B) occurs as a by-product of the regular dye excitation, because during each excitation cycle the molecule crosses to the triplet state with a probability of $p \approx$ 0.05–0.2. Because of its metastability, the triplet state is relatively easily filled up by repeated regular excitation. For saturation, the triplet build-up rate $k_{AB} = p\sigma I$ must be larger than the decay to the S_0, $k_{BA} \approx 10^2$–$10^6 \, \text{s}^{-1}$, which is comparatively slow. Thus, typical I_{sat} is several tens of kW/cm^2, which is 2 to 4 orders of magnitude lower than that with STED. Low I_{sat} is invaluable with regard to the attainable resolution (see equations 2 and 3), and with regard to sample compatibility. The experimental realization of this member of the RESOLFT family will be challenged, however, by the involvement of the triplet state in the photobleaching pathway [43].

The simplest way of realizing a saturated optical transition is to excite the dye intensely [41]. In this case, the ground state S_0 (A) is depleted and the dye expected to reside in the fluorescent state S_1(B). The same RESOLFT formalism applies, except that it is state B that is now fluorescent. State A is depleted such that ultrasharp dark regions are created, which are surrounded

Figure 2
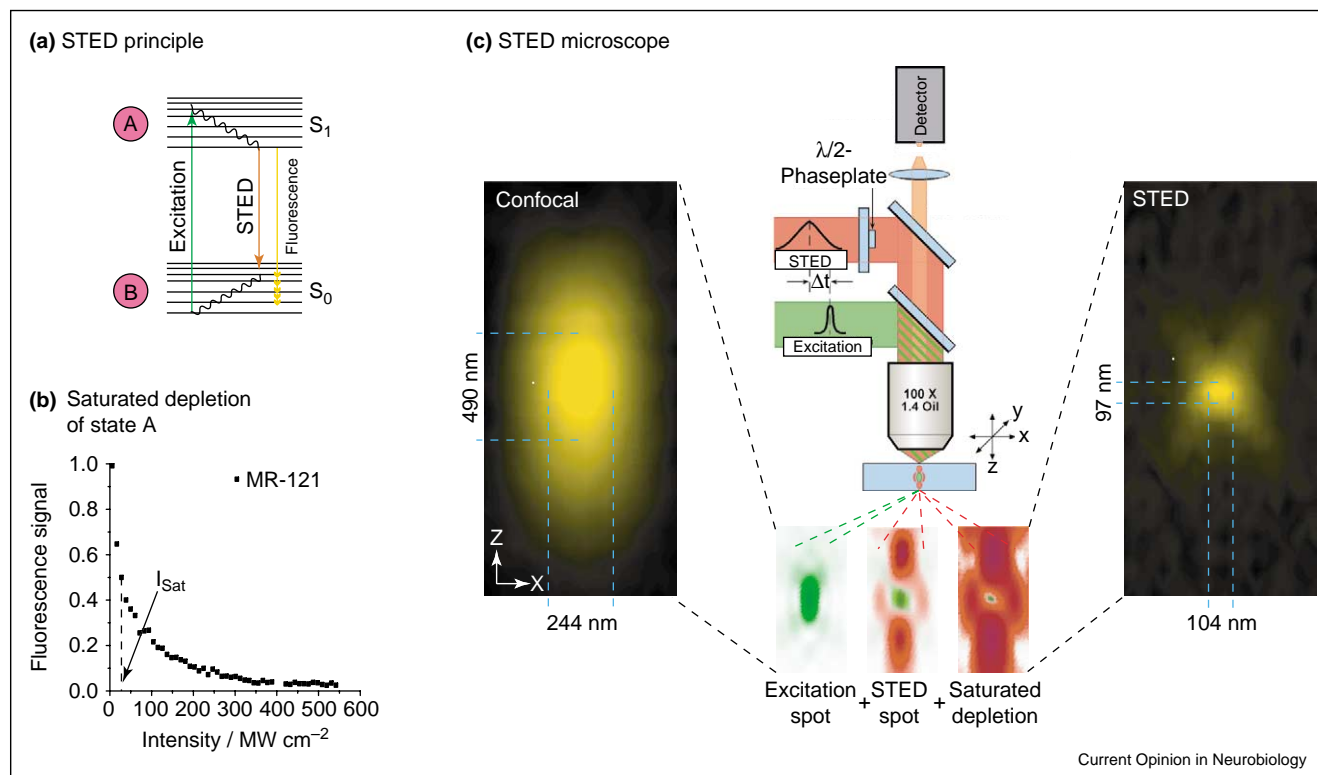
STED-microscopy. **(a)** Molecules in the fluorescent state S_1 (state A) return to the ground state S_0 (state B) by spontaneous fluorescence emission. Return to S_0 might also be optically enforced through stimulated emission. To prevail over the spontaneous emission, stimulated emission depletion of the S_1 requires relatively intense light pulses with durations of a fraction of the S_1 lifetime. **(b)** Saturated depletion of the S_1 with increasing peak intensity of STED pulses of around 100 ps duration, as measured by the remaining fluorescence of a mono-molecular layer of the dye MR-121. For the higher intensity levels, the S_1 is optically depleted. The saturation intensity is defined as the intensity value at which the S_1 is depleted by half. **(c)** In the center of this panel is a schematic of a point scanning STED-microscope. Excitation and STED are accomplished with synchronized laser pulses focused by a lens into the sample, sketched as green and red beams, respectively. Fluorescence is registered by a detector. Intensity distributions in the focus are shown at the bottom: the diffraction limited excitation spot is overlapped with the doughnut shaped STED spot featuring a central zero. Saturated depletion by the STED beam confines the region of excited molecules to the zero leaving a fluorescent spot of subdiffraction dimensions. The images on the left and right depict the confocal and the sub-diffraction-sized spot left by STED, respectively. Note the doubled lateral and fivefold improved axial resolution of STED over confocal microscopy. The reduction in dimensions (x,y,z) yields an ultrasmall volume of subdiffraction dimensions, here 0.67 attoliters, corresponding to an 18-fold reduction in comparison with its confocal counterpart. In spite of using diffraction limited beams, the concept of STED-fluorescence microscopy might, under very favorable conditions, reach spatial resolution at the molecular scale.

by bright fluorescent regions. In a sense, this approach records 'negative' images, which are subsequently made 'positive' by mathematical post-processing. The dark regions can be lines produced by interference patterns, but also 3D-doughnuts. In the latter case, one would produce 'dark 3D-volumes' that are confined by walls of intense fluorescence. The challenges with this otherwise very appealing approach are the mandatory computations that require an excellent signal to noise ratio. As is the situation with STED, excitation saturation competes with fluorescence emission, so that I_{sat} is also given by k_{fl}/σ, which is in the order of 10^{25} photons per cm^2 and second, that is, several tens of MW/cm^2 [17]. Compared with STED, the intensity used for excitation saturation should actually be up to 10 times lower, as the dye can be excited at the maximum of the emission spectrum where

cross-sections are largest. Still, intense excitation increases photobleaching. Relief could be brought by labeling with semiconductor quantum dots [44–46] that do not blink, and to some extent by exciting with pulsed light.

Hence, although the family of RESOLFT concepts is not subject to Abbe's diffraction barrier anymore, the $\sqrt{I/I_{sat}}$ dependence of the resolution gain entails another 'soft barrier', which is the maximum intensity I that the sample or label can tolerate.

A remedy against the need for strong intensities is the implementation of transitions with low values of I_{sat}, that is, optical transitions that are easy to saturate. An example [40,47] is the optical switching of bistable compounds from a fluorescent state (A) into a non-fluorescent state

(B), or vice versa. Optical bistability can be, among others, realized by photo-induced cis-trans isomerization. If both states A and B are (meta)stable, the optical transition A→B or B→A can be completed at very long, if not arbitrary, time scales. Thus, the light energy needed for these transitions can be spread in time [40], reducing I_{sat} to values that are lower by many orders of magnitude as compared to those of STED or the other RESOLFT family members. These processes would also readily lend themselves to parallelization through large area widefield imaging. However, the principal advancement is the insight that nanoscale resolution does not necessarily require large intensities of light [17,39,40].

Suitable candidates for this concept are optically switchable fluorescent proteins. For example, the protein asFP595 can be switched on by green light (B→A) and also switched off (A→B) by blue light recurrently [48,49]. Known candidate proteins, such as asFP595, have major caveats, such as a low quantum efficiency and a strong tendency to form oligomers. These problems could possibly be solved by strategic mutagenesis. Alternatively, new switchable proteins could be found by targeted exploration. A RESOLFT concept based on genetically encoded optically switchable tags is extremely appealing, because it would allow highly specific imaging in live cells with unprecedented optical resolution. We expect that further variants of RESOLFT will emerge in the future.

STED microscopy

STED microscopy is so far the only realized member of the RESOLFT schemes [42,50]. In its initial demonstration, STED microscopy has been realized as a point scanning system, whereby excitation and STED is performed with two synchronized ultrashort pulses (Figure 2c). The first pulse excites the molecule into the fluorescent state S_1 at a suitable wavelength. The immediately succeeding red-shifted second pulse transfers the molecules back to the ground state S_0. The characteristic I_{sat} of several tens of MW/cm^2 scales inversely with the adopted pulse duration of about 10–300 ps. Because the breaking of the diffraction barrier calls for $I_0 \gg I_{sat}$, focal intensities of 100–500 MW/cm^2 are required for typical dyes [37]. For comparison, live cell multiphoton microscopy typically uses 10^3–10^4 times shorter pulses of 10^3–10^4 greater intensity: ∼200 GW/cm^2. Because for pulsed illumination most sample damage mechanisms depend non-linearly on the intensity, the typical values hitherto used for STED have been live cell compatible [42].

Figure 2c shows a typical experimental focal intensity distribution of the excitation spot (green), overlapping with a STED-spot (red) featuring a central hole. Saturated depletion inhibits fluorescence everywhere except for the very center of the focal region [42]. For the $I_0/I_{sat} \approx$ 100 applied for the measurement in Figure 2, the net 3D-spot becomes almost spherical with a diameter of around 100 nm, which amounts to around a sixfold and 2.3 fold increase in axial and lateral resolutions, respectively. Theory would, of course, allow much higher (in principle in the molecular scale) resolution. However, in this experiment the production of a smaller spot was challenged by experimental imperfections [42], such as a finite depth of the central zero, and the increase of photobleaching with increasing I_0/I_{sat}.

The fact that the spot in Figure 2 is squeezed by a greater amount in the z-direction than in the focal plane is due to the higher local intensity of this particular quenching spot along the optic axis. A fivefold improvement of the focal plane resolution over Abbe's barrier has recently been demonstrated with single molecules dispersed on a surface. In combination with linear deconvolution, spots with a FWHM of 28 nm have been reported [51]. Recent experiments also indicate that in accordance with equations (2) and (3), an even higher lateral resolution is possible with STED, provided that photobleaching can be avoided. Because the diffraction barrier is broken, STED-microscopy does not have a firm resolution limit. The attainable resolution solely depends on how well the operational conditions can be realized.

A challenge in the realization is that the spectral window for the STED wavelength might be narrow (10–25 nm), which necessitates screening of the dyes for the most suitable STED wavelength. This in turn calls for pulsed lasers that can be tuned in the visible range. The lack of inexpensive and reliable lasers of this kind has made the implementation of STED relatively cost-intensive. The situation is likely to be alleviated by pulsed laser diodes. In fact, a very compact STED microscope has recently been demonstrated, using a laser diode for the blue excitation and a second diode laser for STED at around 780 nm [52]. As a larger set of wavelengths should become available within the next decade, it should be possible to realize STED microscopy cost-efficiently in the future.

STED microscopy is still in its infancy. So far, most of the applications have been aimed at exploring its principles. Tackling cell biological questions will be a task for the years to come. Strong fluorescence suppression (down to 10%) is conceptually not mandatory, but practically important to attain subdiffraction resolution. Among the first described biological stains that allowed this level of suppression to be reached were lipophilic dyes, such as Styryl 6, 7, and 8, 9M, LDS 751, Pyridine 1, 2, 4 and RH 414, or Oxazine 170 and Nile Red. Because STED was first realized with a Ti:Sapphire laser emitting far-red wavelength (750–800 nm), the emission maximum of these dyes is located around 650–700 nm [42].

Pyridine 4 was used to label the membranes of live *Escherichia coli*. A simultaneous doubling of both the axial and the lateral resolution was observed using a doughnut

mode and STED pulses of around 30 ps duration [42]. This initial improvement will probably be augmented by further optimization of the wavelengths, of the doughnut, and of the pulse duration. Indeed, recent studies revealed that STED related photobleaching dramatically decreased with the duration of the STED pulse, which indicates a strongly nonlinear dependence of bleaching on the STED-pulse intensity [53]. Although bleaching is substantially reduced with pulses of >120 ps duration, more studies are required to address this crucial issue.

In budding yeast, the dye RH 414 is taken up by bulk membrane-internalization and subsequently transported to the vacuolar membrane. The structural integrity of vacuolar membranes is sensitive to many stress factors. Therefore, the subdiffraction resolution imaging of vacuoles in live yeast by STED-microscopy validated that STED-microscopy is amenable to live cell imaging [42].

The principle of STED applies to any fluorophore. Still, not every fluorescent marker can readily be applied without prior investigations. The usually narrow spectral window for efficient STED, which might even change with the chemical environment, has to be established through meticulous screening. Ongoing investigations on fluorescent proteins will establish the operational conditions for STED and its potential with these important labels.

Recently, the resolving power of STED has been synergistically combined with that of 4Pi-microscopy to achieve nanoscale axial resolution [47]. Destructive interference of the counter-propagating spherical wavefronts of the STED pulse at the focal point produces a narrow focal minimum for STED with an axial FWHM of around $\lambda/(4n) \approx 100$–120 nm. Overlap with the regular excitation spot of a single lens has so far rendered focal fluorescence spots down to Δz = 40–50 nm. Linear deconvolution of the data removes the effect of the weak (<30%) sidelobes that accompany the narrow focal spot. Moreover, it further increases the axial resolution to 30–40 nm. This is exemplified in Figures 3 a and b that show axial section (xz-) images of a membrane-labeled *Bacillus megaterium* [47].

The STED-4Pi setup realized so far improves the resolution along the z-axis only, thus rendering a disc-shaped focal spot, whose effect is also noticeable in Figure 3b. The spot could be sculptured down to a spherical shape

Figure 3
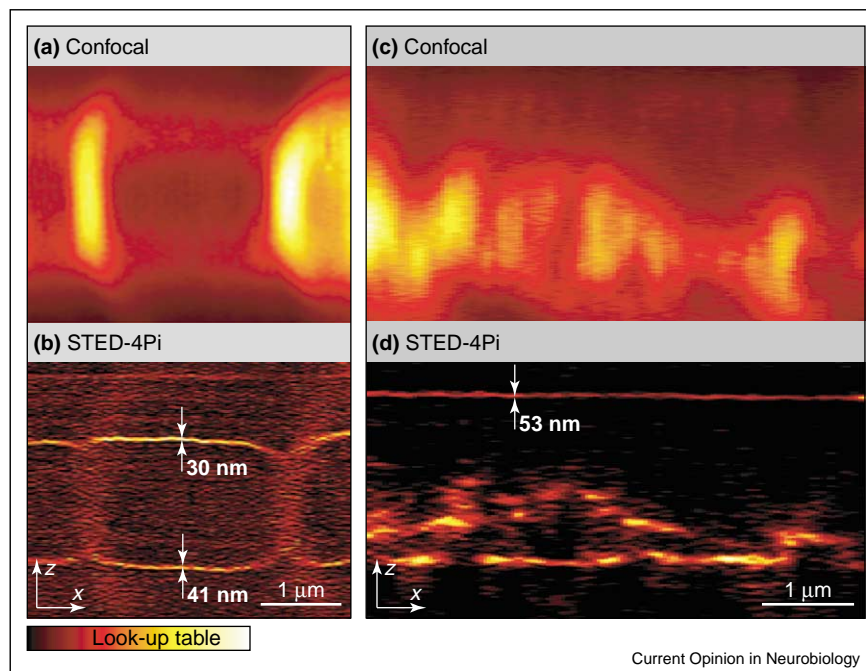
Axial resolution increase provided by STED-4Pi (b,d) over confocal microscopy (a,c). The membranes of a live bacterium (*Bacillus megaterium*) were stained with the dye RH 414 and then simultaneously imaged in the **(a)** confocal and in the **(b)** STED-4Pi microscopy mode. Note that the axial resolution of this focusing microscope is in the order of 30–40 nm. **(c,d)** xz-images from the immunolabeled microtubular network of a human embryonic kidney (HEK)-cell as recorded with a (c) confocal and (d) STED-4Pi-microscope. Both images have been recorded at the same site in the cell. The microtubules were labeled using a primary anti-β-tubulin antibody and a secondary antibody coupled to MR-121. The STED-4Pi images were linearly deconvolved to remove the effect of the 4Pi-sidelobes. Note the straight horizontal line which stems from an MR-121 layer on the cover slip. At this layer, the resolution in the STED-4Pi image is determined as 53 nm. The fixed HEK cells were mounted in aqueous buffer and recorded with water immersion lenses.

Figure 4
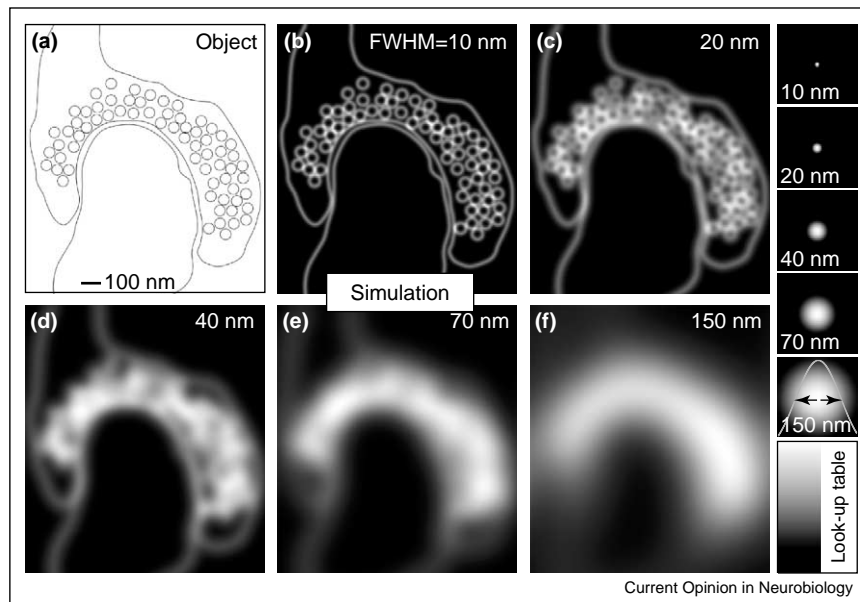
Resolution and visual perception. **(a)** Cartoon of an excitatory synapse drawn to scale from an electron micrograph. The plasma membrane and vesicles of around 50 nm in diameter are shown here. In a real synapse, these membranes could be stained *in vivo* with lipophilic fluorescence dyes. **(b–f)** To assess the effect of the resolution on a putative image, we convolved the cartoon object with sub-diffraction Gaussian foci of 10, 20, 40, 70 and 150 nm diameter. For simplicity, the third dimension (z) is omitted. The simulation indicates that the vesicles can be clearly discerned if the lateral resolution is <20 nm. They are not discernible at resolutions poorer than 40 nm. (f) The resolution of an ideal confocal microscope is in the range of 150 nm. The simulation substantiates the need for a radically greater optical resolution.

by additionally applying a second pulse whose spatial form is designed to squeeze the spot laterally.

STED-4Pi microscopy has also been applied to the imaging of the microtubular cytoskeleton of human embryonic kidney (HEK) cells [54]. The HEK cells were decorated with an anti-β-tubulin antibody and a secondary antibody coupled to the red-emitting dye MR-121. The red-emitting dye displays high STED efficiency (>90%) at a STED-wavelength of around 780–795 nm. Contrary to the confocal xz-sections, in the linearly deconvolved STED-4Pi counterpart, most of the microtubules appear as distinct objects (Figure 3c,d). The attained axial resolution can be inferred from the FWHM of a monomolecular fluorescent layer that has been deposited on the cover slip; it is around 50 nm after linear deconvolution, which corresponds to 1/16 of the irradiation wavelength of 793 nm. It is interesting to note that in the STED-4Pi-image, the brightness of the monomolecular layer is of the same order as that of the microtubules. By contrast, in the confocal image, the layer is overwhelmed by the total signal from the larger focal volume of the confocal microscope. The results obtained with STED and STED-4Pi microscopy demonstrate that the basic physical hurdles have been taken towards attaining a 3D-resolution of the order of a few tens of nanometers.

Outlook

The cartoon in Figure 4 drawn to scale from an electron micrograph, displays the vesicles and the plasma membrane of a simplified excitatory synapse as found in the cortex of the brain [55]. A synaptic vesicle in the presynaptic bouton has a typical diameter of 30–50 nm [56]; its lipid bilayer can be readily labeled with a vital fluorescent dye. We now address the question of what resolution increase is needed to change significantly the perception of the excitatory synapse in the fluorescence microscope. For this purpose we simulated images that would be produced by a fluorescent 'nanoscope' with focal spots of 10–150 nm FWHM (Figure 4).

The simulation is carried out by convolving the structure with the point-spread-function describing the focal spot. For simplicity, we assumed the focal spots to be Gaussian and performed the convolution in two dimensions only. Although 10 nm focal spots give a very faithful representation of the assumed object, at 20 nm the vesicles are already slightly fuzzy, but still discernible. At 40 nm they are indistinct. At a FWHM of 150 nm, which is about the equivalent of the best diffraction limited microscope, no structural information about the vesicular agglomeration can be gained at all. Indeed, synaptic terminals under an epifluorescence microscope reveal little more about their structure than the fact that it is a uniform ring of

fluorescence [57]. The resolution of a confocal or wide-field microscope is not sufficient, even if it is aided by deconvolution. A fundamental change in perception requires a resolution improvement by a factor of 4–5, ideally, by an order of magnitude.

Given the limited rate of excitation and fluorescence emission, high temporal and high spatial resolution might be mutually exclusive in many cases, simply because of the poor statistics of collected photons. High spatial resolution also requires fine spatial sampling, which is not favorable for fast imaging of large areas. Downsizing the region of interest will be inevitable. A remedy is parallelization of the scanning system, either by applying many foci [21] or by utilizing sophisticated structured illumination schemes [29,30,41]. Likewise, the limited number of emission cycles of many fluorophores caps the signal that is available from a sample, and thus, the signal per sample volume. For several staining protocols and applications, the available signal might not match up with the number of collected photons that are required to benefit from the increase in spatial resolution. Therefore, potential improvements in fluorescent labels as well as strategies for avoiding photobleaching will play a vital part in firmly establishing nanoscale resolution in microscopy.

Still, even under poor signal conditions, a RESOLFT method creating ultrasmall focal volumes such as STED might be crucial to techniques that exploit fluorescence statistics. For example, fluorescence correlation spectroscopy [58] depends on small focal volumes to detect rare molecular species or rare molecular interactions in concentrated solutions [59,60]. STED might be the key to attaining nanosized volumes in intact cells. In fact, it is so far the only reported method to squeeze a fluorescence volume to the zeptoliter scale without mechanical confinement [42]. Published results imply the possibility of producing spherical focal volumes of 30 nm diameter [47,51].

Conclusions
The past decade has witnessed the emergence of a family of physical concepts for attaining spatial resolution that is not limited by diffraction. Relying on RESOLFT, the spatial resolution of these concepts is eventually determined by the saturation level that can be realized. Saturation brings about an essential nonlinear relationship between the signal and the applied intensity that allows one to overcome diffraction fundamentally. The nonlinearity brought about by saturation is radically different from that of the well-known multiphoton events. In multiphoton excitation and scattering, the nonlinearity stems from the contemporaneous action of more than one photon, which inevitably demands high focal intensities. By contrast, the nonlinearity brought about by saturated depletion stems from the population kinetics of the involved states. This opens the door to attaining marked nonlinearities even with linear optical transitions, such as single photon excitation and stimulated emission.

Semistable molecular states enable saturable optical transitions at even lower intensities of light. Bistable fluorophore constructs and switchable fluorescent proteins should allow high levels of saturation at low light intensities, which is essential for live cell imaging. This insight might be crucial to opening up the cellular nanoscale with visible light and regular lenses [17,40].

The principle of RESOLFT has been validated through STED microscopy, whose ability to break the diffraction resolution barrier has been experimentally demonstrated. It is worth mentioning that the same strategy of utilizing reversible saturable optical transitions also has the potential to break the diffraction barrier in nanoscale writing and data storage [39,40]. RESOLFT is a physical concept that heavily draws on chemistry, material sciences, and biology. Hence not surprisingly, it has an almost equally large scope. The coming years will show whether or not STED and its RESOLFT cousins are going to establish themselves in biology as part of the microscopic toolbox to elucidate the dynamics and structure of cellular networks.

References and recommended reading

1. Zhang J, Campbell RE, Ting AY, Tsien RY: **Creating new fluorescent probes for cell biology**. *Nat Rev Mol Cell Biol* 2002, **3**:906-918.

2. Lippincott-Schwartz J, Patterson GH: **Development and use of fluorescent protein markers in living cells**. *Science* 2003, **300**:87-91.

3. Abbe E: **Beiträge zur Theorie des Mikroskops und der mikroskopischen Wahrnehmung**. *Arch f Mikroskop Anat* 1873, **9**:413-420.

4. Born M, Wolf E: *Principles of Optics* 7th edn. Cambridge: Cambridge University Press; 2002.

5. König K, Krasieva T, Bauer E, Fiedler U, Berns MW, Tromberg BJ, Greulich KO: **Cell damage by UVA radation of a mercury microscopy lamp probed by autofluorescence modifications, cloning assay, and comet assay**. *J Biomed Opt* 1996, **1**:217-222.

6. Pohl DW, Courjon D: *Near Field Optics*. Dordrecht: Kluwer; 1993.

7. Hell S, Stelzer EHK: **Properties of a 4Pi-confocal fluorescence microscope**. *J Opt Soc Am A* 1992, **9**:2159-2166.

8. Hell SW, Stelzer EHK: **Fundamental improvement of resolution with a 4Pi-confocal fluorescence microscope using two-photon excitation**. *Opt Commun* 1992, **93**:277-282.

9. Nagorni M, Hell SW: **Coherent use of opposing lenses for axial resolution increase in fluorescence microscopy. I. Comparative study of concepts**. *J Opt Soc Am A Opt Image Sci Vis* 2001, **18**:36-48.

10. Lanni F: *Applications of Fluorescence in the Biomedical Sciences* edn 1. Edited by Taylor DL. New York: Liss; 1986.

11. Bailey B, Farkas DL, Taylor DL, Lanni F: **Enhancement of axial resolution in fluorescence microscopy by standing-wave excitation**. *Nature* 1993, **366**:44-48.

12. Nagorni M, Hell SW: **Coherent use of opposing lenses for axial resolution increase in fluorescence microscopy. II. Power and limitation of nonlinear image restoration**. *J Opt Soc Am A Opt Image Sci Vis* 2001, **18**:49-54.

13. Hell SW, Lindek S, Cremer C, Stelzer EHK: **Confocal microscopy with enhanced detection aperture: type B 4Pi-confocal microscopy**. *Opt Lett* 1994, **19**:222-224.

14. Gustafsson MGL, Agard DA, Sedat JW: **Sevenfold improvement of axial resolution in 3D widefield microscopy using two objective lenses**. *Proc SPIE* 1995, **2412**:147-156.

15. Gugel H, Bewersdorf J, Jakobs S, Engelhardt J, Storz R, Hell SW: **Combining 4Pi excitation and detection delivers seven-fold sharper sections in confocal imaging of live cells**. *Biophys J* 2004 in press.

16. Hänninen PE, Hell SW, Salo J, Soini E, Cremer C: **Two-photon excitation 4pi confocal microscope: Enhanced axial resolution microscope for biological research**. *Appl Phys Lett* 1995, **66**:1698-1700.

17. Hell SW: **Toward fluorescence nanoscopy**. *Nat Biotechnol* 2003, **21**:1347-1355.

18. Hell SW, Schrader M, van der Voort HTM: **Far-field fluorescence microscopy with three-dimensional resolution in the 100 nm range**. *J Microsc* 1997, **187**:1-7.

19. Schrader M, Hell SW: **Voort HTMvd: Three-dimensional superresolution with a 4Pi-confocal microscope using image restoration**. *J Appl Phys* 1998, **84**:4033-4042.

20. Blanca CM, Bewersdorf J, Hell SW: **Single sharp spot in fluorescence microscopy of two opposing lenses**. *Appl Phys Lett* 2001, **79**:2321-2323.

21. Egner A, Jakobs S, Hell SW: **Fast 100-nm resolution 3D-microscope reveals structural plasticity of mitochondria in live yeast**. *Proc Natl Acad Sci USA* 2002, **99**:3370-3375.

22. Gustafsson MGL, Agard DA, Sedat JW: **I5M: 3D widefield light microscopy with better than 100 nm axial resolution**. *J Microsc* 1999, **195**:10-16.

23. Bahlmann K, Jakobs S, Hell SW: **4Pi-confocal microscopy of live cells**. *Ultramicroscopy* 2001, **87**:155-164.

24. Egner A, Verrier S, Goroshkov A, Söling H-D, Hell SW: **4Pi-microscopy of the Golgi apparatus in live mammalian cells**. *J Struct Biol* 2004, **147**:70-76.

25. Wilson T, Sheppard CJR: **Theory and Practice of Scanning Optical Microscopy**. New York: Academic Press; 1984.

26. Bertero M, De Mol C, Pike ER, Walker JG: **Resolution in diffraction-limited imaging, a singular value analysis. IV. The case of uncertain localization or non-uniform illumination of the object**. *Opt Acta (Lond)* 1984, **31**:923-946.

27. Bertero M, P. B, Brakenhoff GJ, Malfanti F, Van der Voort HTM: **Three-dimensional image restoration and super-resolution in fluorescence confocal microscopy**. *J Microsc* 1990, **157**:3-20.

28. Neil MAA, Juskaitis R, Wilson T: **Method of obtaining optical sectioning by using structured light in a conventional microscope**. *Opt Lett* 1997, **22**:1905-1907.

29. Heintzmann R, Cremer C: **Laterally modulated excitation microscopy: improvement of resolution by using a diffraction grating**. *SPIE Proc* 1998, **3568**:185-195.

30. Gustafsson MGL: **Surpassing the lateral resolution limit by a factor of two using structured illumination microscopy**. *J Microsc* 2000, **198**:82-87.

31. Gustafsson MGL: **Extended resolution fluorescence microscopy**. *Curr Opin Struct Biol* 1999, **9**:627-634.

32. Cragg GE, So PTC: **Lateral resolution enhancement with standing wave evanescent waves**. *Opt Lett* 2000, **25**:46-48.

33. Pohl DW, Denk W, Lanz M: **Optical stethoscopy: Image recording with resolution λ/20**. *Appl Phys Lett* 1984, **44**:651-653.

34. Betzig E, Chichester RJ: **Single molecules observed by near-field scanning optical microscopy**. *Science* 1993, **262**:1422-1425.

35. Bloembergen N: *Nonlinear optics*. Amsterdam: Benjamin Press; 1965.

36. Hell SW: **Increasing the resolution of far-field fluorescence light microscopy by point-spread-function engineering**. In *Topics in Fluorescence Spectroscopy* 5th Edn. Edited by Lakowicz JR. New York: Plenum Press; 1997:361-422.

37. Hell SW, Wichmann J: **Breaking the diffraction resolution limit by stimulated emission: stimulated emission depletion microscopy**. *Opt Lett* 1994, **19**:780-782.

38. Hell SW, Kroug M: **Ground-state depletion fluorescence microscopy, a concept for breaking the diffraction resolution limit**. *Appl Phys B* 1995, **60**:495-497.

39. Hell SW: **Strategy for far-field optical imaging and writing without diffraction limit**. *Phys Lett A* 2004, **326**:140-145.

40. Hell SW, Jakobs S, Kastrup L: **Imaging and writing at the nanoscale with focused visible light through saturable optical transitions**. *Appl Phys A* 2003, **77**:859-860.

41. Heintzmann R, Jovin TM, Cremer C: **Saturated patterned excitation microscopy- a concept for optical resolution improvement**. *J Opt Soc Am A Opt Image Sci Vis* 2002, **19**:1599-1609.

42. Klar TA, Jakobs S, Dyba M, Egner A, Hell SW: **Fluorescence microscopy with diffraction resolution limit broken by stimulated emission**. *Proc Natl Acad Sci USA* 2000, **97**:8206-8210.

43. Schäfer FP: *Dye Lasers*. Berlin, Heidelberg: Springer; 1973.

44. Alivisatos AP: **Semiconductor clusters, nanocrystals, and quantum dots**. *Science* 1996, **271**:933-937.

45. Peng X, Manna L, Yang W, Wickham J, Scher E, Kadavanich A, Alivisatos AP: **Shape control of CdSe nanocrystals**. *Nature* 2000, **404**:59-61.

46. Bruchez M Jr, Moronne M, Gin P, Weiss S, Alivisatos AP: **Semiconductor nanocrystals as fluorescent biological labels**. *Science* 1998, **281**:2013-2015.

47. Dyba M, Hell SW: **Focal spots of size λ/23 open up far-field fluorescence microscopy at 33 nm axial resolution**. *Phys Rev Lett* 2002, **88**: DOI: 163901.

48. Lukyanov KA, Fradkov AF, Gurskaya NG, Matz MV, Labas YA, Savistky AP, Markelov ML, Zaraisky AG, Zhao X, Fang Y *et al.*: **Natural animal coloration can be determined by a nonfluorescent green fluorescent protein homolog**. *J Biol Chem* 2000, **275**:25879-25882.

49. Chudakov DM, Belousov VV, Zaraisky AG, Novoselov VV, Staroverov DB, Zorov DB, Lukyanov S, Lukyanov KA: **Kindling fluorescent proteins for precise *in vivo* photolabeling**. *Nat Biotechnol* 2003, **21**:191-194.

50. Klar TA, Engel E, Hell SW: **Breaking Abbe's diffraction resolution limit in fluorescence microscopy with stimulated emission depletion beams of various shapes**. *Phys Rev E* 2001, **64**: DOI: 066613.

51. Westphal V, Kastrup L, Hell SW: **Lateral resolution of 28 nm (lambda/25) in far-field fluorescence microscopy**. *Appl Phys B* 2003, **77**:377-380.

52. Westphal V, Blanca CM, Dyba M, Kastrup L, Hell SW: **Laser-diode-stimulated emission depletion microscopy**. *Appl Phys Lett* 2003, **82**:3125-3127.

53. Dyba M, Hell SW: **Photostability of a fluorescent marker under pulsed excited-state depletion through stimulated emission**. *Appl Opt* 2003, **42**:5123-5129.

54. Dyba M, Jakobs S, Hell SW: **Immunofluorescence stimulated emission depletion microscopy**. *Nat Biotechnol* 2003, **21**:1303-1304.

55. Zenisek D, Steyer JA, Almers W: **Transport, capture and exocytosis of single synaptic vesicles at active zones**. *Nature* 2000, **406**:849-854.

56. Hovorka J, Langmeier M, Mares P, Koryntova H: **Synaptic vesicle size and shape profile in the kindling model of epileptogenesis**. *Epilepsy Res* 1997, **28**:225-231.

57. Rouze NC, Schwartz EA: **Continuous and transient vesicle cycling at a ribbon synapse**. *J Neurosci* 1998, **18**:8614-8624.

58. Magde D, Elson EL, Webb WW: **Thermodynamic fluctuations in a reacting system - measurements by fluorescence correlation spectroscopy**. *Phys Rev Lett* 1972, **29**:705-708.

59. Eigen M, Rigler R: **Sorting single molecules: applications to diagnostics and evolutionary biotechnology**. *Proc Natl Acad Sci USA* 1994, **91**:5740-5747.

60. Levene MJ, Korlach J, Turner SW, Foquet M, Craighead HG, Webb WW: **Zero-Mode waveguides for single-molecule analysis at high concentrations**. *Science* 2003, **299**:682-686.